

UC Santa Barbara

UC Santa Barbara Previously Published Works

Title

Tree cover shows strong sensitivity to precipitation variability across the global tropics

Permalink

<https://escholarship.org/uc/item/8711v8wg>

Journal

Global Ecology and Biogeography, 27(4)

ISSN

0960-7447

Authors

Xu, Xiangtao
Medvigy, David
Trugman, Anna T
et al.

Publication Date


2018-04-01

DOI

10.1111/geb.12707

Peer reviewed

Tree cover shows strong sensitivity to precipitation variability across the global tropics

Xiangtao Xu¹  | David Medvigy^{1,2} | Anna T. Trugman³ | Kaiyu Guan⁴ | Stephen P. Good⁵ | Ignacio Rodriguez-Iturbe^{6,7,8}

¹Department of Geosciences, Princeton University, Princeton, New Jersey

²Department of Biological Sciences, University of Notre Dame, Notre Dame, Indiana

³Program in Atmospheric and Oceanic Sciences, Princeton University, Princeton, New Jersey

⁴Department of Natural Resources and Environmental Sciences, University of Illinois at Urbana-Champaign, Urbana, Illinois

⁵Department of Biological & Ecological Engineering, Oregon State University, Corvallis, Oregon

⁶Department of Ocean Engineering, Texas A&M University, College Station, Texas

⁷Department of Civil Engineering, Texas A&M University, College Station, Texas

⁸Department of Agricultural and Biological Engineering, Texas A&M University, College Station, Texas

Correspondence

Xiangtao Xu, Department of Organismic and Evolutionary Biology, Harvard University, Cambridge, MA 02138, USA. Email: xu.withoutwax@gmail.com

Funding information

National Science Foundation, Grant/Award Number: 1151102; Office of Biological and Environmental Research, Grant/Award Number: DE-SC0014363; Texas Engineering Experimental Station; Princeton Environmental Institute (PEI) Walbridge Fund

Editor: Martin Sykes

Abstract

Aim: Vegetation is sensitive to mean annual precipitation (MAP), but the sensitivity of vegetation to precipitation variability (PV) is less clear. Tropical ecosystems are likely to experience increased PV in the future. Here we assessed the importance, magnitude and mechanism of PV effects on tree cover in the context of covarying environmental drivers such as fire, temperature and soil properties.

Location: Tropical land.

Time period: 2000–2010.

Major taxa studied: Trees.

Methods: We compiled climate, soil and remotely-sensed tree cover data over tropical land. We then comprehensively assessed the contribution of PV at different time-scales to tropical tree cover variations and estimated the sensitivity of tree cover to PV changes by conducting rolling-window regression and variance decomposition analyses. We further adopted a mechanistic modelling approach to test whether water competition between trees and grasses can explain the observed effect of PV.

Results: We find that PV contributes 33–56% to the total explained spatial variation (65–79%) in tree cover. The contribution of PV depends on MAP and is highest under intermediate MAP (500–1,500 mm). Tree cover generally increases with rainy day frequency and wet season length but shows mixed responses to inter-annual PV. Based on the estimated sensitivity, tropical tree cover can decrease by 3–5% overall and by up to 20% in Amazonia under a 20% decrease in rainy days. Mechanistic modelling analysis reproduced the continental differences in tree cover along an MAP gradient.

Main conclusions: Under intermediate rainfall regimes (500–1,500 mm), PV can be a more important determinant of tropical tree cover than conventionally proposed drivers such as MAP and fire. The effect of PV likely results from the sensitivity of tree–grass competition to the temporal distribution of water resources. These results show that climate variability can strongly shape the biosphere.

KEYWORDS

biogeography, climate variability, ecohydrology, precipitation variability, tree cover, tree–grass competition, tropical ecology

1 | INTRODUCTION

Over 1 trillion trees grow in tropical and subtropical regions (Crowther et al., 2015), supporting a significant carbon sink and storage (Pan et al., 2011). However, the spatial distribution of tree cover, a widely used measure for tropical tree abundance, is strikingly heterogeneous. This spatial variability defines ecosystems with distinct levels of tree abundances such as grasslands, savannas and forests. These ecosystems provide their own particular sets of ecosystem services, including varying degrees of carbon sequestration, biodiversity, regulation of climate, and support for human socio-economic activities (Chapin, Matson, & Vitousek, 2011; Scholes & Walker, 1993).

Determination of the environmental drivers of spatial variation in tree cover can provide an empirical basis to predict the future fates of tropical ecosystems (Lehmann et al., 2014). In tropical and subtropical ecosystems, water availability has been suggested as the primary determinant on tree cover (Hirota, Holmgren, Van Nes, & Scheffer, 2011; Lehmann et al., 2014; Sankaran et al., 2005; Staver, Archibald, & Levin, 2011a), while other proposed controlling factors include fires, herbivores, and soil properties (Dantas, Hirota, Oliveira, & Pausas, 2016; Lehmann et al., 2014; Sankaran, Ratnam, & Hanan, 2008; Staver, Archibald, & Levin, 2011b). For instance, both *in-situ* (Sankaran et al., 2005) and remotely-sensed (Hirota et al., 2011) observations show that mean annual precipitation (MAP) is strongly correlated with tropical tree cover. However, although precipitation variability (PV) at various time-scales is well known to affect the partitioning of total water supply between trees, grasses, soil evaporation and runoff (Rodriguez-Iturbe & Porporato, 2004; Schaffer, Nordbotten, & Rodriguez-Iturbe, 2015; Xu, Medvigy, & Rodriguez-Iturbe, 2015), PV has received less attention as a determinant of tropical tree cover. PV components such as wet day frequency and seasonality have changed over the course of the 20th century (Feng, Porporato, & Rodriguez-Iturbe, 2013) and they are projected to become more extreme by the end of the 21st century (Easterling et al., 2000; Pascale, Lucarini, Feng, Porporato, & Ul Hasson, 2016; Polade, Pierce, Cayan, Gershunov, & Dettinger, 2014). Therefore, achieving a better understanding of the effects of PV on tree cover is highly relevant in the context of on-going climate change. Existing analyses of the effects of PV have mostly focused on PV at seasonal time-scales using simplistic climatic indices derived from monthly rainfall data (Bucini, Beckage, & Gross, 2017; Holmgren, Hirota, van Nes, & Scheffer, 2013; Lehmann et al., 2014; Staal, Dekker, Xu, & van Nes, 2016; Staver et al., 2011a,b; Zemp et al., 2017; Zeng, Chen, Piao, Rabin, & Shen, 2014) while relatively few studies have investigated the importance of PV at daily (Good & Caylor, 2011; Kulmatiski & Beard, 2013) or inter-annual (Holmgren et al., 2013) time-scales. Moreover, the collinearity and interaction between PV components, MAP and other environmental drivers were not well characterized in previous analyses, which can bias the reported effects and contribution of PV to spatial variations in tree cover.

In this study, we extracted three PV components at different time-scales from pan-tropical daily rainfall data: the wet season length (T_w), the rain-day frequency in the wet season (λ), and the coefficient of variation of annual precipitation (CV_p). We then conducted a

comprehensive statistical analysis on the effects of PV on tree cover, using a wide variety of data sets, including satellite-derived tree cover, mean annual burned area fraction (BAF), topsoil sand fraction, topsoil organic carbon concentration, mean annual temperature (MAT), PV and MAP. We aim to assess (a) the contribution of PV to tropical tree cover variations and (b) the sensitivity of tropical tree cover to PV components with the consideration of the interaction between PV and other environmental factors. We further estimated the changes in tree cover over tropical land under the projected decreases in T_w and λ at the end of this century based on our sensitivity analysis. Finally, we tested the hypothesis that the detected PV effects can largely be explained by tree-grass competition using a biophysical model.

2 | MATERIALS AND METHODS

2.1 | Data source

This study used the Moderate-resolution Imaging Spectroradiometer (MODIS) Vegetation Continuous Fields (VCF) data Collection 5 (MOD44B.005) (DiMiceli et al., 2011; Hansen et al., 2003). We calculated the average tree cover from 2000 to 2010 in the tropics. In order to compare with other environmental data sets, we aggregated the raw VCF data to 0.25° by averaging all tree cover values of the 250 m pixels within the 0.25° grid cell. An earlier analysis showed that this spatial aggregation does not influence the results of statistical analyses with other environmental variables (Staver et al., 2011a) because the variance in tree cover between 0.25° grid cells is 5–10 times higher than the variance within grid cells (Supporting Information Table S1). We calculated the mean annual burned fraction (%/year) at 0.25° resolution from 1996 to 2015 to indicate average fire activity using data from the Global Fire Emission Database v4.0 (Giglio, Randerson, & Van Der Werf, 2013). We extracted topsoil (0–30 cm) sand fraction and soil organic carbon from the gridded Harmonized World Soil Database (Wieder, Boehnert, Bonan, & Langseth, 2014) and MAT from the WorldClim data set (Hijmans, Cameron, Parra, Jones, & Jarvis, 2005). Similar to the MODIS VCF data, the soil and MAT data were also aggregated to 0.25°. Herbivores, especially megafauna like elephants, are also a critical determinant for tropical tree cover (Asner et al., 2009; Hempson et al., 2015). However, fine-resolution global data for herbivore activity are hard to collect and no global gridded data set is available. Thus, we did not include the herbivore effect in our statistical analysis. We extracted MAP and PV (see below for details) from Tropical Rainfall Measuring Mission (TRMM) daily rainfall data (3B42, version 7). This data set provides daily rainfall depth spanning from 50°N to 50°S at 0.25° resolution (Huffman et al., 2007). We used complete annual cycles of daily rainfall from 1999 to 2014.

We limited our analysis to 15°N to 35°S in Africa, America and Australia (Hirota et al., 2011) and excluded grid cells with a high elevation (> 1500 m) and a minimum monthly temperature < 15 °C. This procedure helps to avoid the effect of low temperature on tree growth and thus minimizes the effect of temperature seasonality (Staver et al., 2011b). Elevation and monthly temperature data were extracted from the WorldClim data set (Hijmans et al., 2005). We also excluded grid

cells where anthropogenic land use type (crop, urban or unclassified) was more than 5% of the grid cell area using the MODIS land cover data set (MCD12C1). In addition, we limited our analysis to regions with MAP < 3000 mm. In areas with very high MAP (> 3000 mm), water is almost always abundant. The total number of grid cells included in our statistical analysis is 12,251 for Africa, 10,759 for America, 3,376 for Australia and 26,386 for all the continents together.

All the data were pre-processed to temporal average values before further statistical analysis, because we focused on the average state of tree cover and its sensitivity to climatologically average environmental variables. Therefore, the differences in temporal durations among data sets should have little impacts on our analysis. The spatial maps of all the input data are shown in Supporting Information Figure S1.

2.2 | Calculation of precipitation variability

PV components were extracted from the TRMM data set. First, intra-annual PV includes wet season length (T_w), wet day frequency (λ) and average wet day rain depth (α) in the wet season. These intra-annual PV components are related to MAP as follows:

$$MAP = \frac{\alpha \times \lambda \times T_w}{80\%}. \quad (1)$$

We define T_w to cover 80% of annual rainfall following previous practices (Guan et al., 2014) and therefore, the product of the three intra-annual PV components is equal to 80% of MAP. The four variables in Equation 1 have 3 degrees of freedom. Therefore, we only included MAP, T_w and λ in our analysis.

We estimated T_w for each grid cell using the 16-year average annual cycle of daily rainfall. In order to account for bimodal rainfall, we performed a Fourier Transform on the average annual cycle to extract the dominant rainfall periodicity. We assigned a grid cell as 1-year periodicity if the strength of the 1-year periodicity was stronger than the strength of the half-year periodicity and vice versa (Supporting Information Figure S2). For grid cells with one wet season, we defined the start of a hydrological year as the lowest phase of the 1-year harmonic. We then defined the start (and end) of the wet season as when the cumulative rainfall from the start of a hydrological year crosses 10% (and 90%) of MAP (Guan et al., 2014). T_w was calculated as the time from the start to the end date. For grid cells with two wet seasons, we repeated this algorithm for each half-year cycle and summed up the two individual T_w as total T_w . We estimated λ by assuming that the occurrence of rainfall events is a Poisson stochastic process (Good, Guan, & Caylor, 2015). Therefore, λ was calculated as the total wet days (daily rainfall > 0) in the wet season divided by the total wet season length. Second, we included inter-annual variability of annual precipitation as the inter-annual PV metric in our analysis, which was calculated as the coefficient of variation of annual precipitation (CV_p) during 1999–2014.

2.3 | Statistical analyses

We used three different statistical metrics to investigate the effect and importance of PV for determining the spatial variation in tree cover at

global and continental scales. First, we performed stepwise regression analysis based on K-fold cross-validation. In the regression model, MODIS tree cover is the response variable, and the predictors include MAP, burned area, two soil factors (Sand% and soil organic carbon), and three PV factors (T_w , λ and CV_p). In each step, the variable that reduced root mean square error (RMSE) most following 5-fold cross-validation was selected. Values of the Akaike information criterion (AIC) were also compared with the cross-validation results. We compared two regression models, one with PV (W-PV) in the initial predictor pool and one without PV (N-PV). We calculated the difference in both the R_{adj}^2 and AIC between the two regression models as a metric for the importance of PV. Second, we calculated the standardized regression coefficients (b_{std}) in the W-PV model to infer the sign and size of the effect of each environmental predictor. b_{std} represents the partial sensitivity of tree cover to each predictor. The absolute value of b_{std} is also indicative of variable importance (Grömping, 2015). Third, we calculated a more formal variable relative importance (RI) index based on variance decomposition (Grömping, 2015; Lindeman, Merenda, & Gold, 1980), which is equal to the average of sequential explained variances (SEV) over all possible orderings of each predictor. For a regression model with p different predictors, the average SEV and RI for the variable v is calculated as follows:

$$SEV(v) = \frac{\sum_{i \text{ permutation}} EV(v|i)}{p!}, \quad (2)$$

$$RI(v) = \frac{SEV(v)}{\sum SEV}. \quad (3)$$

In Equation 2, $EV(v|i)$ represents the explained variance by including variable v in the i th permutation of the variable addition sequence. The final RI for variable v is the normalized SEV over all p predictors.

To investigate the nonlinear interaction between PV and MAP, we further extracted data subsets using MAP rolling windows and conducted stepwise regressions using a data subset from each rolling window. We first conducted experiments for different window sizes from 30 to 1000 mm to determine the MAP window size that minimizes the nonlinearity effect but can still provide informative statistical inferences. For each window size, we checked the distribution of sample size and performed twofold cross-validation of the multiple linear regression within each window. We repeated the cross-validation 10 times and calculated the average RMSE. The average RMSE would be high if the window size is large enough to allow for a strong nonlinear effect or if the window size is too small to incorporate sufficient samples for robust regression results. We set the window size to be 200 mm to achieve low cross-validation RMSE and sufficient sample size for most rolling windows (Supporting Information Figure S3). The centre MAP of the windows rolls from 0 to 3000 mm with a step size of 30 mm. Similar to our regression analysis at the continental and global scales, we conducted two stepwise regressions (N-PV and W-PV) within each MAP rolling window and compared the R_{adj}^2 of the two different regression models. To infer the importance of PV and its effect on tree cover, we calculated RI and extracted regression coefficients for each predictor in the W-PV model. The results of the W-PV regressions should not be influenced much by multi-collinearity

because variation inflation factor (VIF) values were all smaller than 10 (Supporting Information Figure S4). We calculated 95% confidence interval for the regression coefficients by multiplying the heteroscedasticity-consistent standard error (HC3_se from the PYTHON package statsmodels.regression.linear_model) by 1.96.

All statistical analyses were performed in PYTHON 2.7.

2.4 | Changes in tree cover under future precipitation variability

While global climate models do not agree on future trends in MAP over tropical land areas, models consistently predict that the frequency of rainy days will decrease (Pascale et al., 2016; Polade et al., 2014). The largest projected changes happen in the eastern part of South America, where rainy days decrease by about 20%. We thus investigate an extreme scenario where across all tropical regions annual wet days are reduced by 20% during the wet season. As the total number of wet days in the wet season is $T_w \times \lambda$, we considered two end-member cases where (a) the reduction of wet days is solely caused by changes in T_w (λ unchanged) and (b) the reduction is solely caused by changes in λ (T_w unchanged). The spatial maps of changes in T_w and λ are displayed in Supporting Information Figure S5.

To calculate the sensitivity of tree cover to T_w and λ for each pixel, we first determined the MAP rolling windows associated with the grid cell (as it is possible for a given grid cell to belong to multiple MAP rolling windows). Then, we calculated the sensitivity to T_w (or λ) as the average of the continent-specific regression coefficient of T_w (or λ) from MAP rolling windows associated with the grid cell. Finally, we computed the potential changes in tree cover as the product of the average regression coefficient for λ (or T_w) and the changes in λ (or T_w).

2.5 | Landscape tree–grass competition modelling

We performed idealistic numerical experiments using a landscape tree–grass competition model coupled with a stochastic rainfall generator (Xu et al., 2015). The model has twenty 10-cm soil layers. For each soil layer, the model tracks the change in soil water at a daily time-scale. Changes in soil water result from infiltration from above (either rainfall or leakage), water extraction from tree and/or grass roots within the layer, soil evaporation and runoff, if applicable, and leakage to the next layer. Plant water extraction is modelled as the current transpiration rate multiplied by the fraction of root biomass in this soil layer while transpiration is calculated as a function of maximum the transpiration rate and soil moisture (Zea-Cabrera, Iwasa, Levin, & Rodríguez-Iturbe, 2006). Evaporation is also calculated as a function of maximum evaporation rate and soil moisture. Leakage is computed following Darcy's law (Xu et al., 2015). The model also tracks net primary production (NPP), which drives the growth of each plant functional type (PFT, tree or grass). NPP is calculated as the product of PFT-specific water use efficiency and daily transpiration. NPP is distributed to leaf, root and stem biomass through an allometric allocation scheme. For root biomass, the model adopts an adaptive biomass allocation scheme over all vertical soil layers. Belowground NPP is allocated to each layer

proportionally to the water extracted from the layer. This adaptive framework can successfully reproduce the observed root distribution at biome level (Schenk, 2008). The model also incorporates shading effects and a water-driven phenology framework. In the model, grasses are more aggressive water users and can suppress tree growth consistent with field observations (February, Higgins, Bond, & Swemmer, 2013; Holdo & Brocato, 2015). However, the relative advantage of grasses over trees depends on the probability of days with high soil moisture and thus will change with PV. Altogether, this model can generate realistic tree–grass coexistence and capture the observed response of tree/grass abundance to precipitation regimes. Details of the model can be found in Xu et al. (2015).

In this study, we conducted two sets of simulations driven by the same observed continental average precipitation statistics. Neither disturbances, soil variation nor temperature were included. In the first set of simulations, we initiated both trees and grass with a leaf area index (LAI) of 1 and a uniform vertical root profile down to 2 m. In the second set of simulations, we only included trees and thus numerically disabled tree–grass competition for water. Everything else was kept the same. We then ran the model for 200 years and extracted the average wet season tree LAI over the last 20 years. The modelling exercise was performed using FORTRAN 90.

3 | RESULTS

3.1 | PV effects on tropical tree cover inferred from statistical analysis

We first assessed the contribution of PV to the spatial variability in tree cover at continental and global scales. A multiple linear regression model that does not include PV (N-PV) accounted for 71% of total spatial variance in tree cover globally, including 73% for Africa, 60% for America and 60% for Australia. The regression with PV variables (W-PV) increased R_{adj}^2 to 79% globally, 78% for Africa, 69% for America and 65% for Australia (Figure 1a–d). Cross-validation and AIC analyses also confirmed that the W-PV model performed better (Table 1). However, the 5–8% increase in R_{adj}^2 does not fully reflect the contribution of PV because of collinearity between variables. Variance decomposition analysis shows that the total variable RI of the three PV predictors reached 56% globally, 46% for Africa, 53% for America and 33% for Australia (Figure 1a–d), values that were higher than the RI values of BAF, MAT and soil variables combined. The results of this RI analysis are also consistent with another metric for variable importance, the absolute values of the standardized regression coefficients (Table 1).

Rolling window regressions show consistent results. The incorporation of PV increased regression R_{adj}^2 by 10–25% in general but the enhancement is insignificant when MAP < 500 mm and peaks at around 1,500 mm globally (Figure 1h). The MAP range with peak PV contribution shifted toward the higher end in Africa and toward the lower end in America, while the pattern in Australia was similar to the global pattern (Figure 1e–g). The RI values of PV further corroborate the results (Figure 1i–l).

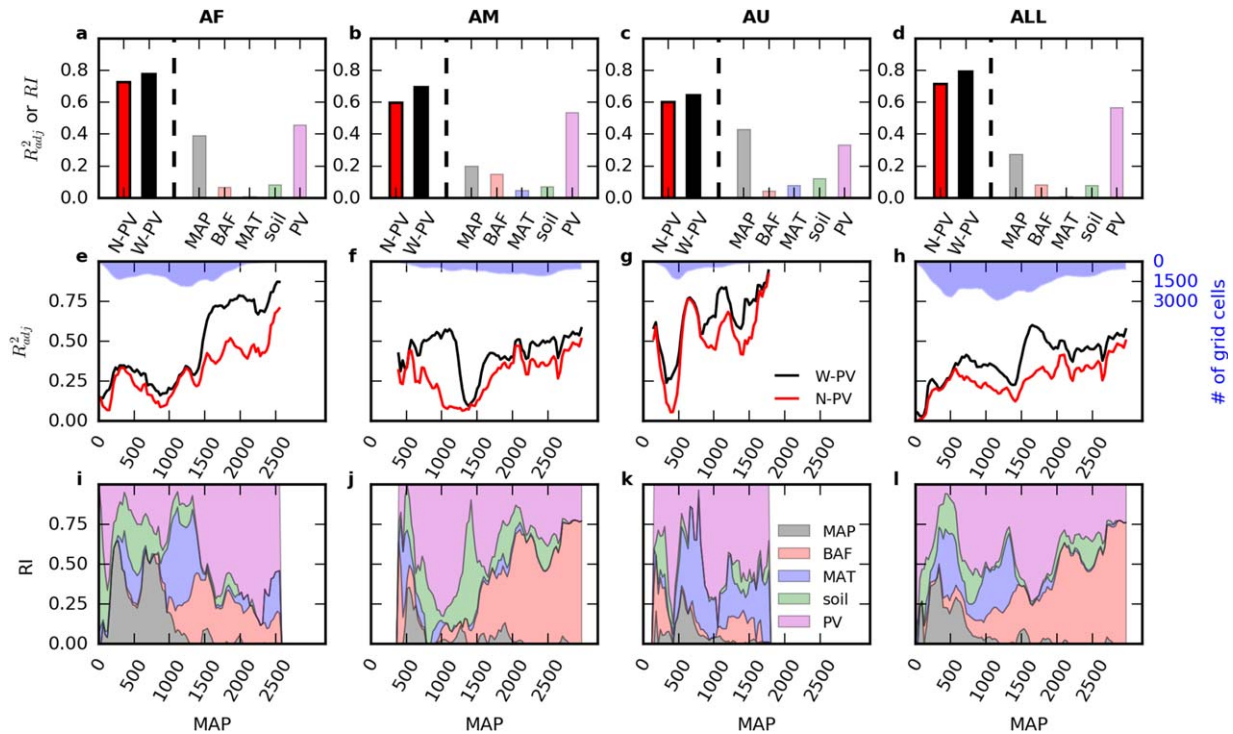


FIGURE 1 Precipitation variability (PV) contributes substantially to variation in tropical tree cover. (a–d) The left side of the dashed line shows the regression model explanatory power (R^2_{adj}) without PV (N-PV, red) and with PV (W-PV, black). The coloured bars on the right-hand side of the dashed line represent the relative importance (RI) of mean annual precipitation (MAP), mean annual burned area fraction (BAF), mean annual temperature (MAT), soil properties including topsoil sand fraction and soil organic carbon concentration (soil), and PV. (e–h) Rolling-window regression R^2_{adj} of the N-PV model (red line) and the W-PV model (black line). Blue shading represents number of grid cells in each rolling window. (i–l) RI of each predictor category from rolling-window regression. AF = Africa; AM = America; AU = Australia

We then investigated the magnitude of the effect of PV on tree cover (Figure 2) by examining the partial sensitivity of tree cover to changes in PV after excluding the effects of MAP, BAF, MAT and soil properties (Supporting Information Figure S6). Across continents, the effect of T_w is consistently positive but varies substantially along a MAP gradient (Figure 2a). The sensitivity to T_w is almost zero in dry regions (MAP < 750 mm), then gradually increases with MAP, peaks at around 1700 mm (1000 mm for American tropics) and slightly declines afterwards. In contrast, the sensitivity to λ varies widely across continents and can even change sign (Figure 2b). The sensitivity to λ is generally negative for low MAP and in Australia while the sensitivity is positive for high MAP and in Africa and America. CV_P also shows mixed effects across continents (Figure 2c). In America, an increase in CV_P in general reduces tree cover while CV_P shows a relatively positive effect on tree cover in Africa and Australia. Overall, the sensitivity of tree cover to T_w and λ dominates the PV effect (Table 1).

3.2 | Responses of tropical tree cover to projected changes in PV

We investigated two scenarios under a 20% decrease in rainy days (Supporting Information Figure S5) where (a) reduction of rainy days is solely caused by changes in λ and (b) the reduction is solely caused by T_w . If only λ was changed (first scenario), tree cover would on average reduce by c. 1.68% in Africa and 6.64% in America but increase by

1.07% in Australia (Figure 3a–c). The tree cover increase in Australia is caused by the negative sensitivity of tree cover to λ (Figure 2b). Summed over all continents, 36% of our study region would experience more than 5% tree cover reduction (Figure 3d). In the second scenario where T_w was changed, tree cover would consistently decrease by 2 to 8% on average across continents. 52% of our study region would experience a > 5% tree cover reduction in this scenario. The maximum reduction can reach 20% in equatorial Africa and southern Amazonia (Supporting Information Figure S7).

3.3 | Simulated tree abundance from tree-grass competition model

From remote-sensing observations, average tree cover under the same MAP increases from Australia to Africa and America, especially when rainfall is between 500 and 1000 mm (Figure 4a). This pattern is largely consistent with continental differences in T_w , which increases from Australia to Africa and America when MAP > 500 mm (Figure 4e). Meanwhile, Africa has the highest BAF and λ , America has the lowest BAF and λ and Australia lies in between (Figure 4d,f). We only show continental differences of these three environmental drivers because they contribute most to the variations in tropical tree cover (Table 1).

Simulations driven solely by continental T_w and λ values along an MAP gradient (Figure 4e,f) produced similar continental patterns of tree abundance indicated by equilibrium LAI (Figure 4b). Moreover, the

TABLE 1 Stepwise regression results and variable importance analysis for data from all three continents

ALL			
Regression model		AIC	R ²
TC ~ MAP + T _w + λ + fire + CV _p + Sand% + MAT + SOC		215,207.1	0.792
TC ~ MAP + fire + MAT + Sand% + SOC		223,872.4	0.713
Variable	b _{std}	RI (%)	VIF
MAP	0.18	27.1	6.26
Fire	-0.22	8.0	1.42
MAT	0.02	0.5	1.18
Sand%	-0.02	1.8	1.21
SOC	0.02	6.0	1.49
λ	0.32	14.8	5.20
T _w	0.42	28.0	3.05
CV _p	-0.04	13.8	3.46
AF			
Regression model		AIC	R ²
TC ~ MAP + T _w + fire + Sand% + SOC + MAT + λ		95,108.2	0.775
TC ~ MAP + fire + Sand% + SOC		97,530.6	0.726
Variable	b _{std}	RI (%)	VIF
MAP	0.55	39.1	7.22
Fire	-0.21	6.4	1.46
MAT	-0.02	0.5	1.26
Sand%	0.09	1.1	1.26
SOC	0.03	7.1	1.69
λ	0.04	13.1	5.37
T _w	0.33	32.7	2.65
CV _p	n.a.	n.a.	n.a.
AM			
Regression model		AIC	R ²
TC ~ MAP + fire + CV _p + T _w + λ + Sand% + MAT + SOC		87,913.6	0.694
TC ~ MAP + fire + Sand% + MAT + SOC		90,895.3	0.596
Variable	b _{std}	RI (%)	VIF
MAP	-0.09	20.0	5.69
Fire	-0.28	14.9	1.12
MAT	0.06	4.7	1.36
Sand%	-0.11	3.8	1.11
SOC	0.02	3.1	1.24
λ	0.45	19.5	3.88
T _w	0.43	21.4	3.42
CV _p	-0.05	12.6	2.46
AU			
Regression model		AIC	R ²
TC ~ MAP + T _w + fire + λ + SOC + MAT + CV _p + Sand%		21,550.0	0.645
TC ~ MAP + MAT + fire + SOC + Sand%		21,984.4	0.602
Variable	b _{std}	RI (%)	VIF
MAP	1.23	43.0	10.14
Fire	-0.21	4.2	2.67
MAT	-0.13	7.8	2.51
Sand%	0.04	0.4	1.34
SOC	0.17	11.5	1.51
λ	-0.57	16.6	19.3
T _w	0.11	8.2	3.13
CV _p	-0.06	8.3	3.75

RI = relative importance; AF = Africa; AM = America; AU = Australia; MAP = mean annual precipitation; MAT = mean annual temperature; SOC = soil organic carbon; TC = tree cover; λ = the rain-day frequency in the wet season; T_w = wet season length; CV_p = coefficient of variation of annual precipitation.

Note. For each continent, the first two rows show the regression R²_{adj} and Akaike information criterion (AIC) with (W-PV) and without precipitation variability (N-PV). Predictors are arranged based on the selection sequence of forward stepwise regression. The standardized regression coefficient (b_{std}), variable relative importance based on variance decomposition (RI) and variance inflation factor (VIF) are listed for the regression model with PV.

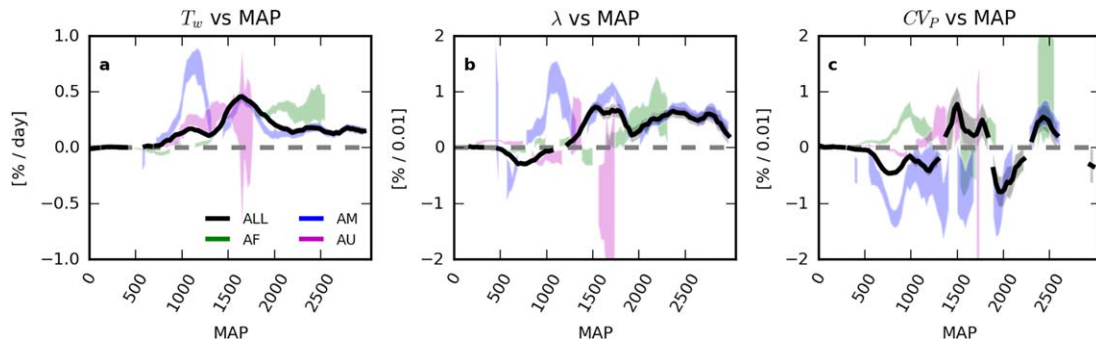


FIGURE 2 The sensitivity of tree cover to precipitation variability depends on mean annual precipitation (MAP). (a–c) Multiple regression coefficients of wet season length (T_w , a), wet day frequency (λ , b) and rainfall inter-annual variability (CV_p , c) as a function of the centre of MAP rolling windows. Black lines represent results that incorporate data from all three continents. Coloured shading represents the 95% confidence interval with the consideration of heteroscedasticity for each continent (green – Africa, blue – America and magenta – Australia). The missing values indicate that the variable was not selected by stepwise regression in those rolling windows. Regression coefficients of other predictors included in the regression are shown in Supporting Information Figure S6. AF = Africa; AM = America; AU = Australia

continental difference in the simulated LAI disappeared when grasses were excluded from the simulations (Figure 4c).

4 | DISCUSSION

4.1 | PV as a determinant of tropical tree cover

Our statistical analysis shows that MAP is the first-order controlling factor over tropical tree cover, consistent with previous studies (Hirota et al., 2011; Sankaran et al., 2005), but also reveals that PV contributes significantly to the spatial variations in tropical tree cover in addition to MAP, fire, and soil effects (Table 1, Figure 1). From an ecological perspective, PV should be most important in intermediate MAP regions where the temporal distribution of water resource matters most. Indeed, our regression results show that the RI of PV (Figure 1) peaks

at intermediate rainfall. Across the global tropics, when MAP is low, total rainfall is the dominant determinant of tree cover while fire effect is most important when MAP is very high (Figure 1). There are also continental differences in the pattern of PV effects. In Africa, the MAP value of peak PV contribution became higher (Figure 1). In addition, environmental factors show much lower explanatory power for tree cover variations in Africa compared with the other two continents (Figure 1e–g). This is possibly because herbivores (unaccounted for in our statistical models) play a bigger role in determining tree abundance when $MAP < 1500$ mm (Dantas et al., 2016; Hempson et al., 2015), and megafauna are more abundant in Africa than elsewhere. In contrast, the MAP value of peak PV contribution is lower in the American tropics because fire effect became dominant at high MAP (Figure 1j). The effects of fire in the American tropics can be rather strong in terms of shaping ecosystem structure (Supporting Information Figure S6b)

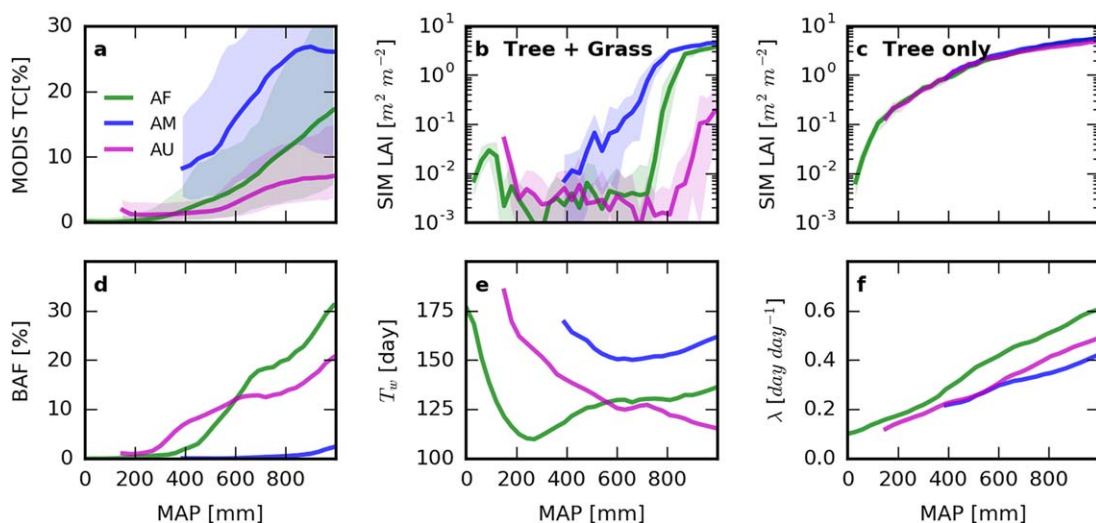


FIGURE 3 Continental differences in tree cover are explained by tree–grass competition. The average values of Moderate-resolution Imaging Spectroradiometer (MODIS) tree cover (TC; a) within each mean annual precipitation (MAP) rolling window are compared with the simulated equilibrium tree leaf area index (SIM LAI) in log-scale from simulations with competition from grass (b) and without competition (c) for Africa (green), America (blue) and Australia (magenta). The average values of mean annual burned area fraction (BAF; d), wet season length (T_w ; e), wet day frequency (λ ; f) within each MAP rolling window are shown for each continent. AF = Africa; AM = America; AU = Australia

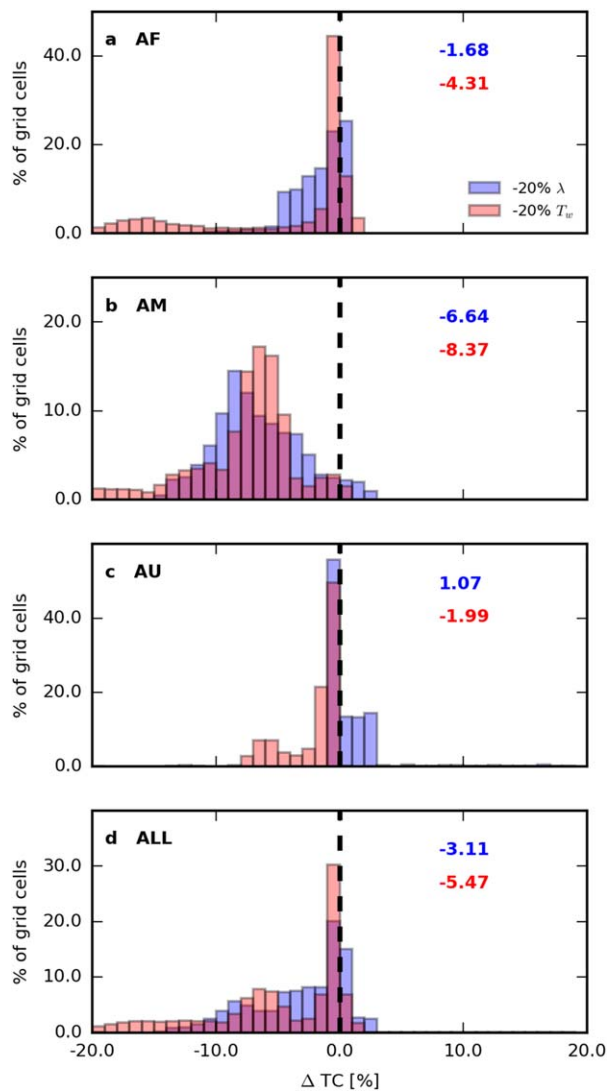


FIGURE 4 Large potential decreases in tree cover (TC) under projected reduction of rainy days. Histograms of potential tree cover change under two scenarios – a 20% reduction in wet day frequency (λ ; blue) and a 20% reduction in wet season length (T_w ; red) are shown for tropics in Africa (a), America (b), Australia (c) and all three continents (d). Average tree cover change is shown in upper right corner of each panel. AF = Africa; AM = America; AU = Australia

despite the fact that the frequency of fires can be low (Supporting Information Figure S1), probably because trees in the Amazon have thinner barks compared with other tropical areas (Pellegrini et al., 2017) and thus are more vulnerable to fire.

PV can determine tree cover through different ecological pathways. Intra-annual PV such as T_w and λ can influence the temporal distribution of plant soil water stress and thus influence tree performance (Rodríguez-Iturbe & Porporato, 2004). For instance, longer T_w allows for less seasonal water stress and longer growing seasons for trees (Guan et al., 2014). At inter-annual time-scales, large fluctuations in annual rainfall can bring extreme droughts that severely damage trees (Phillips et al., 2009) as well as wet pulses that facilitate tree seedlings' escape from the demographic bottleneck and create new canopies

(Holmgren et al., 2013; Sankaran, Ratnam, & Hanan, 2004). Our results suggest that the benefits of wet pulses may be dominant in the African and Australian tropics while the damage from droughts dominates in the American tropics. In addition, PV can interact with other climate factors shaping tropical ecosystems such as fire. Longer dry seasons and infrequent rainfall events can favour the occurrence of fires that reduce tree cover (Hanson et al., 2016; Lehmann et al., 2014; Staver et al., 2011b; Van Der Werf, Randerson, Giglio, Gobron, & Dolman, 2008).

4.2 | Tree-grass competition explains the PV effects on tree cover

Tree-grass competition can play a critical role in determining the structure and dynamics of tropical ecosystems, especially for savannas (Sankaran et al., 2004; Scholes & Walker, 1993). Trees and grasses differ drastically in various structural and functional traits, leading to distinctive water use strategies. Field experiments have shown that the presence of grasses can greatly impact tree performance (February et al., 2013; Holdo & Brocato, 2015). Previous theoretical modelling analysis has also shown that tropical C_4 grasses, which usually have an aggressive water use strategy, have a competitive advantage over trees when rainfall comes as intense but infrequent pulses because these grasses can obtain a large share of water within a short period of time (Xu et al., 2015). Using the same theoretical tree-grass competition model, we show that the observed continental differences in tree cover were reproduced in the model only when tree-grass competition was included (Figure 4). Meanwhile, this continental difference in tree cover contradicts variations in continental fire regime because BAF is higher in Africa compared with Australia (Figure 4d), which suggests that fire is unlikely to explain the continental patterns of tree cover.

One challenge to the tree-grass competition theory is that the reported response of tree-grass competition to λ variations differs substantially among studies. Trees have been reported to benefit from either increased (Good & Caylor, 2011) or decreased λ (Kulmatiski & Beard, 2013). In this study, the effect of λ on tree cover also shows opposite signs across continents and the MAP gradient (Figure 2b). Here we argue that such mixed effects are because tree cover response to λ can result from complex tree-grass competition processes. High λ can benefit trees over grasses because grasses are aggressive water users and better at exploiting intense but less frequent rainfall when grasses and trees have similar rooting depths (Xu et al., 2015). However, high λ can also favour shallow-rooted grasses over deep-rooted trees because less water can seep into deeper soil layers (Kulmatiski & Beard, 2013; Sankaran et al., 2004). The overall effect of λ on tree cover is probably contingent on the rooting profiles of trees and grasses. Rooting profiles of both trees and grasses in tropical ecosystems are correlated with total rainfall, rainfall seasonality and soil texture (Schenk & Jackson, 2002a). However, trees develop shallower roots under more seasonal rainfall while grass rooting depth is relatively insensitive to rainfall seasonality (Schenk & Jackson, 2002b). We thus expected that the effect of λ on tree cover depends more strongly on T_w , compared with MAP and the topsoil sand fraction.

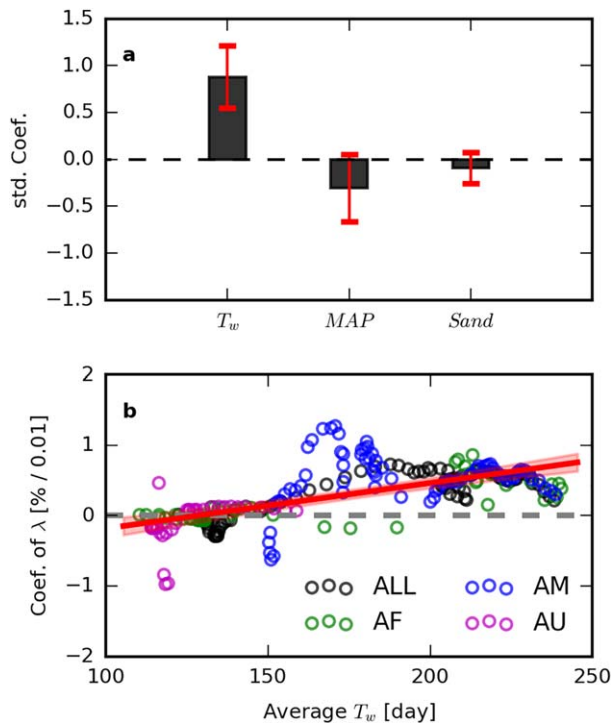


FIGURE 5 Multiple regression results of the effect of wet day frequency (λ) on tree cover. (a) The sensitivity of tree cover to λ from rolling-window regressions was regressed against the average wet season length (T_w), mean annual precipitation (MAP) and sand fraction of grid cells within each MAP rolling window ($n = 239$). Black bars show the standardized regression coefficients of the multiple regression. Red error bars represent 95% confidence interval. Only the coefficient of T_w is significantly different from zero. (b) The regression coefficient of λ linearly increases with the average T_w value of each MAP rolling window. Only coefficients significantly different from 0 are shown. Colour of each dot denotes the continent of the MAP window. Red line and shading shows the linear regression result and 95% confidence interval, respectively. AF = Africa; AM = America; AU = Australia

We further performed a multiple regression over the sensitivity of tree cover to λ (regression coefficients shown in Figure 2b) against the average MAP, T_w , and topsoil sand fraction within each rolling window. We combined global and continental regression results but only included rolling windows where the sensitivity of tree cover to λ is significantly different from zero. In total, 239 rolling windows were selected. The regression results confirmed this expectation and show that the sensitivity of the effect of λ on tree cover to T_w is positive and significantly different from zero while the sensitivity of the effect of λ on tree cover to MAP and the topsoil sand fraction is not significantly different from zero (Figure 5a). Moreover, our analysis implies that a significant positive effect of increased λ on tree cover occurs when T_w is longer than c. 150 days (Figure 5b). Interestingly, the study that reports a negative effect was conducted in South Africa (Kulmatiski & Beard, 2013) with T_w similar to or shorter than 150 days (Supporting Information Figure S1) while a positive effect was reported for a pan-African analysis (Good & Caylor, 2011) that covers a wider range of T_w values. These results provide

additional evidence that the response of tropical ecosystems to PV is driven by tree–grass competition.

5 | CONCLUSIONS

The on-going climate changes include not only the changes in mean state but also changes in variability. Such changes in environmental variability can exert significant impacts on terrestrial ecosystems even if the average environmental state does not change because ecosystem responses to environment are often nonlinear (Knapp et al., 2008; Medvigy, Wofsy, Munger, & Moorcroft, 2010). While it is widely known that precipitation extremes such as drought can catastrophically disturb tropical ecosystems (Doughty et al., 2015; Phillips et al., 2009), we here demonstrate that tree abundance can respond to a spectrum of PV, which is likely driven by tree–grass competition. Our results help to explain the spatial patterns of tropical tree abundance and also provide novel insights into the fate of tropical tree cover and ecosystem structure under future climate projections with empirical estimates of ecosystem sensitivity to PV. We further show that tropical tree cover will likely suffer from the projected changes in PV, which may reduce or even cancel the beneficial effect of the concurrent increases in atmospheric CO_2 concentration (Higgins & Scheiter, 2012; Stevens et al., 2016). It is also noteworthy that changes in PV can also affect tree cover indirectly through interacting with other environmental factors such as fire (Hantson et al., 2016), which requires further research from field experiments and data synthesis. Altogether, our work highlights the importance of accurately monitoring and predicting PV for understanding future vegetation dynamics and carbon cycles in the tropics.

ACKNOWLEDGMENTS

D.M. gratefully acknowledges support from National Science Foundation award 1151102 and US Department of Energy, Office of Science, Office of Biological and Environmental Research, Terrestrial Ecosystem Science (TES) Program award DE-SC0014363. I.R.-I. gratefully acknowledges the support of the Texas Engineering Experimental Station (TEES). A.T.T. is supported by the Princeton Environmental Institute (PEI) Walbridge Fund and a National Science Foundation Graduate Research Fellowship. The authors thank the Princeton Institute for Computational Science and Engineering (PICSciE) for computational support and Kelly Heilman, Jason McClachlan and two anonymous referees for their helpful comments.

DATA ACCESSIBILITY

The data that support the findings of this study are publicly available online at glcf.umd.edu/data/, pmm.nasa.gov, fuoco.geog.umd.edu, www.worldclim.org and daac.ornl.gov. Model codes are available at <https://github.com/xiangtao-princeton/PrecVarTreeGrass/>.

CONFLICT OF INTEREST

The authors declare no competing financial interests.

ORCID

Xiangtao Xu  <http://orcid.org/0000-0002-9402-9474>

REFERENCES

- Asner, G. P., Levick, S. R., Kennedy-Bowdoin, T., Knapp, D. E., Emerson, R., Jacobson, J., ... Martin, R. E. (2009). Large-scale impacts of herbivores on the structural diversity of African savannas. *Proceedings of the National Academy of Sciences USA*, 106(12), 4947–4952. <https://doi.org/10.1073/pnas.0810637106>
- Bucini, G., Beckage, B., & Gross, L. J. (2017). Climate seasonality, fire and global patterns of tree cover. *Frontiers of Biogeography*, 9(2), e33610. <https://doi.org/10.21425/F59233610>
- Chapin, F. S., Matson, P. A., & Vitousek, P. M. (2011). *Principles of terrestrial ecosystem ecology* (2nd ed.). New York: Springer.
- Crowther, T. W., Glick, H. B., Covey, K. R., Bettigole, C., Maynard, D. S., Thomas, S. M., ... Bradford, M. A. (2015). Mapping tree density at a global scale. *Nature*, 525(7568), 201–205. <https://doi.org/10.1038/nature14967>
- Dantas, V. de L., Hirota, M., Oliveira, R. S., & Pausas, J. G. (2016). Disturbance maintains alternative biome states. *Ecology Letters*, 19(1), 12–19. <https://doi.org/10.1111/ele.12537>
- DiMiceli, C., Carroll, M., Sohlberg, R., Huang, M. C., Hansen, M. C., & Townsend, J. R. G. (2011). *Annual global automated MODIS vegetation continuous fields (MOD44B) at 250 m spatial resolution for data years Beginning Day 65, 2000–2010, Collection 5*. College Park, MD: University of Maryland.
- Doughty, C. E., Metcalfe, D. B., Girardin, C. A. J., Amezquita, F. F., Cabrera, D. G., Huasco, W. H., ... Malhi, Y. (2015). Drought impact on forest carbon dynamics and fluxes in Amazonia. *Nature*, 519(7541), 78–82. <https://doi.org/10.1038/nature14213><http://www.nature.com/nature/journal/v519/n7541/abs/nature14213.html#supplementary-information>
- Easterling, D. R., Meehl, G. A., Parmesan, C., Changnon, S. A., Karl, T. R., & Mearns, L. O. (2000). Climate extremes: Observations, modeling, and impacts. *Science*, 289(5487), 2068–2074. <https://doi.org/10.1126/science.289.5487.2068>
- February, E. C., Higgins, S. I., Bond, W. J., & Swemmer, L. (2013). Influence of competition and rainfall manipulation on the growth responses of savanna trees and grasses. *Ecology*, 94(5), 1155–1164. <https://doi.org/10.1890/12-0540.1>
- Feng, X., Porporato, A., & Rodriguez-Iturbe, I. (2013). Changes in rainfall seasonality in the tropics. *Nature Climate Change*, 3(9), 811–815. <https://doi.org/10.1038/nclimate1907>
- Giglio, L., Randerson, J. T., & Van Der Werf, G. R. (2013). Analysis of daily, monthly, and annual burned area using the fourth-generation global fire emissions database (GFED4). *Journal of Geophysical Research: Biogeosciences*, 118(1), 317–328. <https://doi.org/10.1002/jgrg.20042>
- Good, S. P., & Caylor, K. K. (2011). Climatological determinants of woody cover in Africa. *Proceedings of the National Academy of Sciences USA*, 108(12), 4902–4907. <https://doi.org/10.1073/pnas.1013100108>
- Good, S. P., Guan, K., & Caylor, K. K. (2015). Global patterns of the contributions of storm frequency, intensity, and seasonality to inter-annual variability of precipitation. *Journal of Climate*, 29, 3–15. <https://doi.org/10.1175/jcli-d-14-00653.1>
- Grömping, U. (2015). Variable importance in regression models. *Wiley Interdisciplinary Reviews: Computational Statistics*, 7, 137–152. <https://doi.org/10.1002/wics.1346>
- Guan, K., Good, S. P., Caylor, K. K., Sato, H., Wood, E. F., & Li, H. (2014). Continental-scale impacts of intra-seasonal rainfall variability on simulated ecosystem responses in Africa. *Biogeosciences*, 11(23), 6939–6954.
- Hansen, M. C., DeFries, R. S., Townshend, J. R. G., Carroll, M., Dimiceli, C., & Sohlberg, R. A. (2003). Global percent tree cover at a spatial resolution of 500 meters: First results of the MODIS vegetation continuous fields algorithm. *Earth Interactions*, 7(10), 1–15. [https://doi.org/10.1175/1087-3562\(2003\)007<0001:GPTCAA>2.0.CO;2](https://doi.org/10.1175/1087-3562(2003)007<0001:GPTCAA>2.0.CO;2)
- Hantson, S., Arneith, A., Harrison, S. P., Kelley, D. I., Prentice, I. C., Rabin, S. S., ... Yue, C. (2016). The status and challenge of global fire modelling. *Biogeosciences*, 13(11), 3359–3375. <https://doi.org/10.5194/bg-13-3359-2016>
- Hempson, G. P., Archibald, S., & Bond, W. J. (2015). A continent-wide assessment of the form and intensity of large mammal herbivory in Africa. *Science*, 350(6264), 1056–1061. <https://doi.org/10.1126/science.aac7978>
- Higgins, S. I., & Scheiter, S. (2012). Atmospheric CO₂ forces abrupt vegetation shifts locally, but not globally. *Nature*, 488(7410), 209–212. <https://doi.org/10.1038/nature11238>
- Hijmans, R. J., Cameron, S. E., Parra, J. L., Jones, P. G., & Jarvis, A. (2005). Very high resolution interpolated climate surfaces for global land areas. *International Journal of Climatology*, 25(15), 1965–1978. <https://doi.org/10.1002/joc.1276>
- Hirota, M., Holmgren, M., Van Nes, E. H., & Scheffer, M. (2011). Global resilience of tropical forest and savanna to critical transitions. *Science*, 334(6053), 232–235. Retrieved from <http://www.sciencemag.org/content/334/6053/232>
- Holdo, R., & Brocato, E. (2015). Tree–grass competition varies across select savanna tree species: A potential role for rooting depth. *Plant Ecology*, 216(4), 577–588. <https://doi.org/10.1007/s11258-015-0460-1>
- Holmgren, M., Hirota, M., van Nes, E. H., & Scheffer, M. (2013). Effects of interannual climate variability on tropical tree cover. *Nature Climate Change*, 3(8), 755–758. <https://doi.org/10.1038/nclimate1906>
- Huffman, G. J., Bolvin, D. T., Nelkin, E. J., Wolff, D. B., Adler, R. F., Gu, G., ... Stocker, E. F. (2007). The TRMM multisatellite precipitation analysis (TMPA): Quasi-global, multiyear, combined-sensor precipitation estimates at fine scales. *Journal of Hydrometeorology*, 8(1), 38–55. <https://doi.org/10.1175/JHM560.1>
- Knapp, A. K., Beier, C., Briske, D. D., Classen, A. T., Luo, Y., Reichstein, M., ... Weng, E. (2008). Consequences of more extreme precipitation regimes for terrestrial ecosystems. *BioScience*, 58(9), 811–821. <https://doi.org/10.1641/B580908>
- Kulmatiski, A., & Beard, K. H. (2013). Woody plant encroachment facilitated by increased precipitation intensity. *Nature Climate Change*, 3(9), 833–837. <https://doi.org/10.1038/nclimate1904>
- Lehmann, C. E. R., Anderson, T. M., Sankaran, M., Higgins, S. I., Archibald, S., Hoffmann, W. A., ... Bond, W. J. (2014). Savanna vegetation–fire–climate relationships differ among continents. *Science*, 343(6170), 548–552. <https://doi.org/10.1126/science.1247355>
- Lindeman, R. H., Merenda, P. F., & Gold, R. Z. (1980). *Introduction to bivariate and multivariate analysis*. Glenview, IL: Scott Foresman.
- Medvigy, D., Wofsy, S. C., Munger, J. W., & Moorcroft, P. R. (2010). Responses of terrestrial ecosystems and carbon budgets to current and future environmental variability. *Proceedings of the National Academy of Sciences USA*, 107(18), 8275–8280. <https://doi.org/10.1073/pnas.0912032107>
- Pan, Y., Birdsey, R. A., Fang, J., Houghton, R., Kauppi, P. E., Kurz, W. A., ... Hayes, D. (2011). A large and persistent carbon sink in the world's

- forests. *Science*, 333(6045), 988–993. <https://doi.org/10.1126/science.1201609>
- Pascale, S., Lucarini, V., Feng, X., Porporato, A., & Ul Hasson, S. (2016). Projected changes of rainfall seasonality and dry spells in a high greenhouse gas emissions scenario. *Climate Dynamics*, 46(3–4), 1331–1350.
- Pellegrini, A. F. A., Anderegg, W. R. L., Paine, C. E. T., Hoffmann, W. A., Kartzinel, T., Rabin, S. S., ... Knops, J. (2017). Convergence of bark investment according to fire and climate structures ecosystem vulnerability to future change. *Ecology Letters*, 20(3), 307–316. <https://doi.org/10.1111/ele.12725>
- Phillips, O. L., Aragao, L. E. O. C., Lewis, S. L., Fisher, J. B., Lloyd, J., Lopez-Gonzalez, G., ... Torres-Lezama, A. (2009). Drought sensitivity of the Amazon rainforest. *Science*, 323(5919), 1344–1347. <https://doi.org/10.1126/science.1164033>
- Polade, S. D., Pierce, D. W., Cayan, D. R., Gershunov, A., & Dettinger, M. D. (2014). The key role of dry days in changing regional climate and precipitation regimes. *Scientific Reports*, 4(1), 4364–48pp. <https://doi.org/10.1038/srep04364>
- Rodriguez-Iturbe, I., & Porporato, A. (2004). *Ecohydrology of water-controlled ecosystems: Soil moisture and plant dynamics*. United Kingdom: Cambridge University Press. Retrieved from <http://www.loc.gov/catdir/toc/cam041/2004046566.html>
- Sankaran, M., Hanan, N. P., Scholes, R. J., Ratnam, J., Augustine, D. J., Cade, B. S., ... Zambatis, N. (2005). Determinants of woody cover in African savannas. *Nature*, 438(7069), 846–849. <https://doi.org/10.1038/nature04070>
- Sankaran, M., Ratnam, J., & Hanan, N. P. (2004). Tree–grass coexistence in savannas revisited – insights from an examination of assumptions and mechanisms invoked in existing models. *Ecology Letters*, 7(6), 480–490. <https://doi.org/10.1111/j.1461-0248.2004.00596.x>
- Sankaran, M., Ratnam, J., & Hanan, N. (2008). Woody cover in African savannas: The role of resources, fire and herbivory. *Global Ecology and Biogeography*, 17(2), 236–245. <https://doi.org/10.1111/j.1466-8238.2007.00360.x>
- Schaffer, B. E., Nordbotten, J. M., & Rodriguez-Iturbe, I. (2015). Plant biomass and soil moisture dynamics: Analytical results. *Proceedings of the Royal Society A: Mathematical, Physical and Engineering Sciences*, 471(2183), 20150179. <https://doi.org/10.1098/rspa.2015.0179>
- Schenk, H. J. (2008). The shallowest possible water extraction profile: A null model for global root distributions. *Vadose Zone Journal*, 7(3), 1119. <https://doi.org/10.2136/vzj2007.0119>
- Schenk, H. J., & Jackson, R. B. (2002a). Rooting depths, lateral root spreads and below-ground/above-ground allometries of plants in water-limited ecosystems. *Journal of Ecology*, 90(3), 480–494. <https://doi.org/10.1046/j.1365-2745.2002.00682.x>
- Schenk, H. J., & Jackson, R. B. (2002b). The global biogeography of roots. *Ecological Monographs*, 72(3), 311–328. <https://doi.org/10.2307/3100092>
- Scholes, R. J. J., & Walker, B. H. B. H. (1993). *An African Savanna: Synthesis of the Nylsvley Study*. Cambridge studies in applied ecology and resource management (1st ed.). United Kingdom; Cambridge University Press. Retrieved from <https://doi.org/10.1017/CBO9780511565472>
- Staal, A., Dekker, S. C., Xu, C., & van Nes, E. H. (2016). Bistability, spatial interaction, and the distribution of tropical forests and savannas. *Ecosystems*, 19(6), 1080–1091. <https://doi.org/10.1007/s10021-016-0011-1>
- Staver, A. C., Archibald, S., & Levin, S. (2011a). Tree cover in sub-Saharan Africa: Rainfall and fire constrain forest and savanna as alternative stable states. *Ecology*, 92(5), 1063–1072. <https://doi.org/10.1890/10-1684.1>
- Staver, A. C., Archibald, S., & Levin, S. A. (2011b). The global extent and determinants of savanna and forest as alternative biome states. *Science*, 334(6053), 230–232. <https://doi.org/10.1126/science.1210465>
- Stevens, N., Erasmus, B. F. N., Archibald, S., Bond, W. J., O'Connor, T., Puttick, J., ... Gandar, M. (2016). Woody encroachment over 70 years in South African savannas: Overgrazing, global change or extinction aftershock? *Philosophical Transactions of the Royal Society B: Biological Sciences*, 371(1703), 67–88. <https://doi.org/10.1098/rstb.2015.0437>
- Van Der Werf, G. R., Randerson, J. T., Giglio, L., Gobron, N., & Dolman, A. J. (2008). Climate controls on the variability of fires in the tropics and subtropics. *Global Biogeochemical Cycles*, 22(3), GB3028. <https://doi.org/10.1029/2007GB003122>
- Wieder, W. R., Boehnert, J., Bonan, G. B., & Langseth, M. (2014). *Regridded harmonized world soil database v1.2*. Oak Ridge, TN: ORNL Distributed Active Archive Center. Retrieved from <https://doi.org/10.3334/ORNLDAAC/1247>
- Xu, X., Medvigy, D., & Rodriguez-Iturbe, I. (2015). Relation between rainfall intensity and savanna tree abundance explained by water use strategies. *Proceedings of the National Academy of Sciences USA*, 112(42), 12992–12996. <https://doi.org/10.1073/pnas.1517382112>
- Zea-Cabrera, E., Iwasa, Y., Levin, S., & Rodriguez-Iturbe, I. (2006). Tragedy of the commons in plant water use. *Water Resources Research*, 42(6), W06D02. <https://doi.org/10.1029/2005wr004514>
- Zemp, D. C., Schleussner, C.-F., Barbosa, H. M. J., Hirota, M., Montade, V., Sampaio, G., ... Rammig, A. (2017). Self-amplified Amazon forest loss due to vegetation-atmosphere feedbacks. *Nature Communications*, 8, 14681. <https://doi.org/10.1038/ncomms14681>
- Zeng, Z., Chen, A., Piao, S., Rabin, S., & Shen, Z. (2014). Environmental determinants of tropical forest and savanna distribution: A quantitative model evaluation and its implication. *Journal of Geophysical Research: Biogeosciences*, 119(7), 1432–1445. <https://doi.org/10.1002/2014JG002627>

BIOSKETCHES

XIANGTAO XU is an ecologist with interest in understanding how environment especially water interacts with vegetation dynamics. His research involves integrating ecological observations and ecological modelling to understand terrestrial ecosystem responses to environmental change.

DAVID MEDVIGY is interested in how climate variability affects the functioning, structure and composition of terrestrial ecosystems.

SUPPORTING INFORMATION

Additional Supporting Information may be found online in the supporting information tab for this article.

How to cite this article: Xu X, Medvigy D, Trugman AT, Guan K, Good SP, Rodriguez-Iturbe I. Tree cover shows strong sensitivity to precipitation variability across the global tropics. *Global Ecol Biogeogr*. 2018;27:450–460. <https://doi.org/10.1111/geb.12707>